International Journal of Fatigue 31 (2009) 1788–1794

Contents lists available at ScienceDirect

International Journal of Fatigue

journal homepage: www.elsevier.com/locate/ijfatigue

The effect of load ratio on fatigue life and crack propagation behavior of an extruded magnesium alloy

S. Ishihara [a,*], A.J. McEvily [b], M. Sato [a], K. Taniguchi [a], T. Goshima [a]

[a] Department of Mechanical Engineering, University of Toyama, 3190 Gofuku, Toyama 930-8555, Japan
[b] Institute of Materials Science, University of Connecticut, CT, USA

ARTICLE INFO

Article history:
Received 12 September 2008
Received in revised form 26 January 2009
Accepted 17 February 2009
Available online 27 February 2009

Keywords:
Fatigue
Magnesium alloy
Stress ratio
S–N curves
Crack propagation

ABSTRACT

Fatigue experiments were carried out in laboratory air using an extruded magnesium alloy, AZ31, to investigate the effect of load ratio on the fatigue life and crack propagation behavior. The crack propagation behavior was analyzed using a modified linear elastic fracture mechanics parameter, *M*. The relation crack propagation rate vs. *M* parameter was found to be useful in predicting fatigue lives at different *R* ratios. Good agreement between the estimated and the experimental results at each stress ratio was obtained.

1. Introduction

Magnesium alloys are candidates as structural materials due to their high specific strength and good damping capacity [1]. For example, when they are used as car parts, weight saving of the car body and reduction of fuel consumption can be expected, since they are the lightest among metals. Further, a better driving feeling can be obtained because oscillation of the car body can be reduced due to their good damping capacity. However, before utilizing magnesium alloys for machines and structures, a determination of fatigue lives and crack propagation behavior of the alloys at different load ratios is required.

There already have been a number of investigations concerning the fatigue properties of magnesium alloys. For example, Goodenberger and Stephens [2] have provided basic information concerning the fatigue behavior of the cast magnesium alloy, AZ91E-T6 in laboratory air. Hilpert and Wagner [3] have carried out experiments to determine the degree of degradation in fatigue resistance due to corrosion of the AZ80 magnesium alloy as a function of various surface treatments such as electro-polishing, grinding, machining and shot peening. Eisenmeier et al. [4] have studied the fatigue behavior of AZ91 magnesium alloy that had been processed using a vacuum die casting method. They reported that the fatigue cracks were initiated at casting defects in the material, and that the crack growth behavior was influenced by the microstructure of the material. Shih et al. [5] performed fatigue experiments on the extruded magnesium alloy AZ61A, and reported that fatigue cracks were initiated at surface or near-surface inclusions, and that the initial crack growth behavior was affected by the microstructure.

Until now, empirical relations, Gerber and Goodman diagrams have been utilized for evaluation of the effect of mean stress on fatigue lives, however, theoretical methods to analyze the effect of *R* ratios on the fatigue lives are very few and limited. McEvily et al. [6] proposed a modified linear elastic fracture mechanics approach. This method was originally developed to analyze both the long through and short fatigue crack propagation behavior. Then the method was shown to be able to predict crack growth behavior under multiple two-step loading condition [7] and in different materials [8–9].

In the present study, fatigue tests were conducted on an extruded magnesium alloy to investigate fatigue lives (*S–N* curves) and crack propagation behavior under different stress ratios, *R*. The modified linear elastic fracture mechanics approach was applied to analyze the crack propagation behavior of the extruded magnesium alloy AZ31 and to predict *S–N* curves at different *R* ratios. Comparison between experimental and calculated results reveals that the approach proposed by McEvily et al. [6] is effective and useful in analyzing the short fatigue crack propagation behavior at different *R* ratios including negative *R* ratios.

* Corresponding author. Tel./fax: +81 76 445 6771.
E-mail address: ishi@eng.u-toyama.ac.jp (S. Ishihara).

0142-1123/$ - see front matter © 2009 Elsevier Ltd. All rights reserved.
doi:10.1016/j.ijfatigue.2009.02.034

2. Material, specimens and experimental procedures

2.1. Material

The extruded magnesium alloy AZ31 was used in this investigation. Its chemical composition is listed in Table 1. A cylindrical billet with a diameter of 200 mm was extruded into a round bar with a diameter of 70 mm, an extrusion ratio of 10. Table 2 lists the extrusion conditions under which the alloy was processed. Fig. 1 shows the microstructure of the material used in the present study. The average grain diameter of the material after extrusion was 9 μm, and its aspect ratio was about 0.8.

2.2. Experimental procedures

2.2.1. Specimens and fatigue testing machine

In the present study two types of fatigue tests were used. Rotating bending fatigue tests ($R = -1$) at 30 Hz and axial-load fatigue tests at 10 Hz were conducted in laboratory air at room temperature at stress ratios, $R = 0.1$, -1, and -2. Fig. 2a and b shows the specimen shapes and dimensions of the rotating bending fatigue tests and axial fatigue tests, respectively. For the rotating bending fatigue tests, round bar specimens with a minimum diameter of 5.6 mm were used (stress concentration factor 1.04). For the axial-load tests, round bar specimens with a minimum diameter of 4 mm were used (stress concentration factor 1.06). The specimen surfaces were polished to a mirror-like finish using emery papers and diamond paste prior to fatigue tests to eliminate any effect of the roughness of the specimen surface on the fatigue results, and to facilitate the observations of crack propagation on the specimen surfaces. Monotonic tension and compression tests were also conducted using a similar specimen as shown in Fig. 1b. Its gauge length was 5 mm.

2.2.2. Fatigue crack propagation tests

2.2.2.1. Short surface crack. The propagation rates of the short surface cracks that initiated and propagated on the specimen surfaces during both the rotating bending fatigue process and the axial fatigue process were investigated using the replication technique. Fatigue tests were interrupted at a constant interval during the fatigue process to obtain the replicas of the specimen surfaces. Crack lengths recorded on the replicas were determined with an optical microscope at a magnification of 400. For calculations of the stress intensity factor, K, the following expression was used [10]

$$K = Y\sigma\sqrt{\pi a}, \quad (1)$$

where σ is stress, a is a half crack length, and Y is a crack-shape correction factor with a value of 0.73 [11] given by assuming that a crack-shape is semi-circular.

2.2.2.2. Long through crack. Besides the crack propagation behavior of the short surface crack, crack propagation behavior of the long through crack was also investigated using the round type compact tension specimens as shown in Fig. 3. Crack lengths were measured using a travelling microscope at a magnification of 40.

The following expression [12] was used for calculations of the stress intensity factor, K

$$K = \frac{P}{tW^{1/2}} \times \frac{(2+\alpha)(0.76 + 4.8\alpha - 11.58\alpha^2 + 11.43\alpha^3 - 4.08\alpha^4)}{(1-\alpha)^{3/2}}, \quad (2)$$

where $\alpha = a/W$, a is a crack length, and W is a specimen width.

Crack opening stress intensity factor, K_{op} during a loading cycle was determined based on the unloading elastic compliance method [13] by affixing strain gauges ahead of the crack tip.

Table 1
Chemical compositions of the material used (wt%).

Al	Zn	Mn	Fe	Si	Cu	Ni
3.10	0.79	0.35	0.0041	0.019	0.0023	0.0008

Table 2
Extrusion conditions.

Extrusion temperature	Extrusion speed	Extrusion ratio
573 K	2 m/min	10

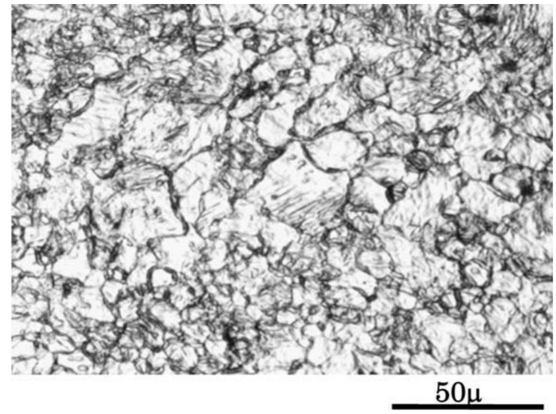

Fig. 1. Microstructure of the material AZ31 used in the present study.

3. Experimental results

3.1. Monotonic tension and compression tests

Fig. 4 shows the stress vs. strain relationships for both tension and compression tests. As can be seen from the figure, the yield strength under compression is lower than that for tension. Table 3 lists the mechanical properties of the material under tension and compression tests. In the compression tests, the specimen (4.5 mm in diameter and 8 mm in gauge length) used failed due to buckling at the maximum compressive load. A similar result was also reported by Muller and Muller [14]. They suggested [14] that twinning is concerned with the above difference between the yield strength in tension and the one in compression, but a detailed mechanism is unknown at present.

3.2. Fatigue tests

3.2.1. S–N curves

Fig. 5a and b shows S–N curves for the different R ratios, $R = 0.1$, -1 and -2. Those results were obtained from the axial fatigue tests and also from the rotating bending (RB) fatigue tests. In Fig. 5a and b, the maximum stress $\sigma_{\max}$ and stress amplitude σ_a are taken as the vertical axes, respectively. Similar S–N curves between the axial fatigue tests and the rotating bending fatigue tests are seen. S–N curves for $R = -1$ and $R = -2$ bend at 10^5–10^6 cycles. From Fig. 5a, the maximum stress $\sigma_{\max}$ at a constant fatigue life decreases with a decrease in the value of R.

However, in Fig. 5b, the reverse is true, i.e., the stress amplitude σ_a at a constant fatigue life increases with a decrease in the R value.

The relationship between stress amplitude σ_a and mean stress σ_m was drawn using the data from Fig. 5. Fig. 6 shows the results.